

Adhesive protein-free synthetic hydrogels for retinal pigment epithelium cell culture with low ROS level

Yong Mei Chen,^{1,2} Zhen Qi Liu,^{1,2} Zhi Hui Feng,³ Feng Xu,^{2,3} Jian Kang Liu³

¹Department of Chemistry, School of Science, MOE Key Laboratory for Non-Equilibrium Synthesis and Modulation of Condensed Matter, Xi'an Jiaotong University, Xi'an 710049, People's Republic of China

²Biomedical Engineering and Biomechanics Center, Xi'an Jiaotong University, Xi'an 710049, People's Republic of China

³Center for Mitochondrial Biology and Medicine, The Key Laboratory of Biomedical Information Engineering of Ministry of Education, School of Life Science and Technology and Frontier Institute of Life Science, FIST, Xi'an Jiaotong University, Xi'an 710049, People's Republic of China

Received 23 June 2013; accepted 24 July 2013

Published online 14 August 2013 in Wiley Online Library (wileyonlinelibrary.com). DOI: 10.1002/jbm.a.34904

Abstract: Engineering of human retinal pigment epithelium (RPE) cell monolayer with low level of reactive oxygen species (ROS) is important for regenerative RPE-based therapies. However, it is still challenging to culture RPE monolayer with low ROS level on soft substrates *in vitro*. To address this, we developed cytocompatible hydrogels to culture human RPE cell monolayer for future use in regenerative RPE-based therapies. The cell adhesion, proliferation, monolayer formation, morphology, survival, and ROS level of human ARPE-19 cells cultured on the surfaces of negatively charged poly(2-acrylamido-2-methyl propane sulfonic sodium) (PNaAMPS) and neutral poly(*N,N*-dimethylacrylamide) (PDMAAm) hydrogels with different stiffness were investigated. The impor-

tance of hydrogel stiffness on the cell function was firstly highlighted on the base of determined optimal Young's modulus for cultivation of RPE cell monolayer with relatively low ROS level. The construction of RPE cell monolayer with low ROS level on the PNaAMPS hydrogel may hold great potential as promising candidates for transplantation of RPE cell monolayer-hydrogel construct into the subretinal space to repair retinal functions. © 2013 Wiley Periodicals, Inc. *J Biomed Mater Res Part A*: 102A: 2258–2267, 2014.

Key Words: hydrogel, retinal pigment epithelium cell, reactive oxygen species, Young's modulus

How to cite this article: Chen YM, Liu ZQ, Feng ZH, Xu F, Liu JK. 2014. Adhesive protein-free synthetic hydrogels for retinal pigment epithelium cell culture with low ROS level. *J Biomed Mater Res Part A* 2014;102A:2258–2267.

INTRODUCTION

Retinal pigment epithelium (RPE) cells are located between choroid capillaries and the neurosensory retina as an intermediary. *In vivo*, the RPE cells pack together like cobblestones to form a compacted monolayer that rests on a basement membrane above Bruch's membrane.^{1,2} This strategic position allows RPE cells to perform highly specialized roles in the maintenance of retinal homeostasis and visual function, such as phagocytosing spent rod, supporting photoreceptor cell functions, transporting nutrients, and metabolites as well as synthesizing glycosaminoglycans.^{3–5} Because of the important functions of retina, the degeneration or dysfunction of RPE cells can result in various retinal diseases which is implicated in visual disability including

retinitis pigmentosa and age-related macular degeneration (ARMD), especially, ARMD is currently the leading cause of blindness in the developed world.^{6–8} For most of the cases, the treatment of these diseases requires transplantation of RPE cell monolayer. However, potential donors are very limited, and there is an urgent need of RPE cell monolayer for tissue engineering.

Strategy of tissue-engineered RPE cell monolayer based on *in vitro* culture of RPE cells on substrates has been developed for transplantation of RPE cell-substrate construct into the subretinal space.^{3,9,10} The substrates act as suitable supportive matrix for RPE cells to proliferate and form monolayer. Besides, the substrate should closely mimic the native cell microenvironment, such as biomechanical

Correspondence to: Y. M. Chen; e-mail: chenym@mail.xjtu.edu.cn or J. K. Liu; e-mail: j.liu@mail.xjtu.edu.cn

Contract grant sponsor: National Natural Science Foundation of China; contract grant numbers: 51073127, 51173144

Contract grant sponsor: the Research Fund for the Doctoral Program of Higher Education of China; contract grant number: 2010-0201110040

Contract grant sponsors: Scientific Research Foundation for the Returned Overseas Chinese Scholars, State Education Ministry, the Fundamental Research Funds for the Central Universities; contract grant number: 2009-0109-08140018

Contract grant sponsor: International Science & Technology Cooperation Program Supported by Ministry of Science and Technology of China and Shaanxi Province; contract grant number: 2013KW14-02

Contract grant sponsor: New Research Support Project of Xi'an Jiaotong University, P. R. China; contract grant number: 2009-08141001

Contract grant sponsor: the Major International Joint Research Program of China; contract grant number: 11120101002

Contract grant sponsor: International Science & Technology Cooperation Program of China; contract grant number: 2013DFG02930

and physicochemical properties.¹¹ Hydrogels, a representative soft and wet material, have similar properties (e.g., ~90% in water content, ~kPa in Young's modulus) with soft tissues, which can mimic the native extracellular matrix of multicellular organisms.^{12,13} Furthermore, the properties of three-dimensional (3D) hydrogel networks are close to the Bruch's membrane, such as capability for transportation of oxygen, nutrients, and metabolites.^{14,15} Based on the aforementioned advantages, both nature derived hydrogels (e.g., collagen and gelatin)^{14,16} and synthetic hydrogels [e.g., poly(*N*-isopropylacrylamide) and poly (methacrylate-*co*-meth acrylamide)]^{9,17,18} have been explored as promising materials for RPE cell cultivation and transplantation.

Native RPE cells are situated in a microenvironment with the highest oxygen tensions of the body and produce large amount of reactive oxygen species (ROS) when playing their physiological functions, such as in the process of phagocytosis.¹⁹ Besides, accumulating evidences have demonstrated that RPE cells can easily suffer from oxidative damage which eventually leads to a variety of retinal diseases.^{20,21} In the blindness caused by ARMD, high intracellular concentration of ROS is thought to be a major factor to induce cell undergoing death pathway by reacting with almost any organic molecule such as DNA, RNA, lipid, carbohydrate, or protein.²² Therefore, an ideal substrate should be rationally designed for the formation of human RPE cell monolayer with low ROS level. However, the existing studies have not paid any attention to this, and little is known regarding the oxidative stress of the RPE cells cultured on hydrogel substrates.

Although various hydrogel based substrates have been developed for mimicking cell microenvironment, these substrates need modification by cell-adhesive proteins (e.g., fibronectin and laminin) and short-chain peptides.^{9,12,23,24} Compared to modified substrates, the approach without modification offers several advantages, such as capability to directly analyze cell-substrate interaction by adjusting physicochemical properties of hydrogels, good reproducibility, free of infection, tolerance for high-temperature sterilization, and relatively low cost.²⁵ We have previously cultivated various cell lines on synthetic hydrogels requiring no modification of any adhesive proteins or peptides, including endothelial cells (ECs),²⁵⁻²⁹ rabbit synovial tissue derived fibroblast cells,²⁶ human articular chondrocytes,³⁰ murine chondrogenic ATDC5 cells,³¹ and mouse embryonic stem cells (mESCs).³² It is found that hydrogels with high charge density facilitate ECs and STDFCs to form cell monolayers, as well as accelerate spontaneous differentiation of embryoid bodies of mESCs into three germ layers. Moreover, we have found that neutral hydrogels are suitable for spontaneous redifferentiation of dedifferentiated human chondrocytes into chondrocytes, as well as for differentiation of ATDC5 cell into chondrocytes. However, the effect of physicochemical properties of these modification-free hydrogels on the ROS level and behaviors of RPE cells has not been explored yet.

In this contribution, we developed a new approach based on adhesive protein-free synthetic hydrogels for human RPE cell cultivation with low ROS level. We investigated the effects

of chemical structure and Young's modulus (E) of modification-free synthetic hydrogels on human RPE cell adhesion, proliferation, viability, monolayer formation, and ROS level. A spontaneously immortalized adult human RPE cell line, ARPE-19 cells, was used as an *in vitro* model for RPE cells, because the cells display many morphological and functional features similar to native adult human RPE cells.^{33,34} It was found that soft PNaAMPS hydrogels with Young's modulus of 5.0 ± 0.2 kPa and 24.0 ± 1.0 kPa were suitable for cultivation of human RPE cell monolayer with low ROS level.

MATERIALS AND METHODS

Materials

In this study, we used poly (2-acrylamido-2-methyl propane sulfonic sodium) (PNaAMPS) and poly (*N,N*-dimethylacrylamide) (PDMAAm) hydrogels as substrates for RPE cell cultivation, where PNaAMPS hydrogel has proved cytocompatibility,^{27,28} and PDMAAm hydrogel has been used as material for contact lenses.³⁵ Negatively charged monomer NaAMPS was prepared following the previous report.²⁷ Neutral monomer DMAAm (Tokyo Kasei Kogyo, Tokyo, Japan), cross-linking agent, *N,N'*-methylenebisacrylamide (MBAA, Tokyo Kasei Kogyo, Tokyo, Japan) and initiator, 2-oxoglutaric acid (Wako Pure Chemicals, Osaka, Japan), were all used as purchased. The structure of chemicals is shown in Figure 1(A).

Hydrogel synthesis

Negatively charged PNaAMPS hydrogel and neutral PDMAAm hydrogels with different crosslinking concentration (C) used as cell substrates were synthesized by radical polymerization of as previous reported.²⁵ The gelation was performed in the precleaned glass molds with a 10×10 mm² silicone rubber spacer with thickness of 0.5 mm or 2 mm to obtain sheet-shaped hydrogels. After 1M monomer (NaAMPS or DMAAm), 2–10 mol % cross-linker (MBAA) and 0.1 mol % initiator (2-oxoglutaric acid) in respect to the monomer concentration were dissolved into ion-exchanged water, the reaction solution was poured into the glass mold, then the mold was irradiated with UV light (wavelength, 365 nm) for polymerization at room temperature (12 h). The thickness of PBS-equilibrated hydrogels synthesized in glass molds with 0.5 mm and 2 mm thickness is about 0.5–0.75 mm and about 2–3 mm, respectively. Thick hydrogels were used for hydrogel characterization and cell cultivation, and thin hydrogels with large ratio of surface area and lateral area were used for test of protein adsorption. Prepared sheet-shaped hydrogels were subsequently immersed in ion-exchanged water for 3 days to extract residual chemicals that did not react during the gelation. The hydrogels are denoted as water-equilibrated hydrogels. The water-equilibrated hydrogels were then immersed into phosphate buffer solution (PBS) to adjust the pH and ionic strength of the solution containing in the hydrogels to 7.0 and about 0.15M, respectively. The hydrogels are denoted as PBS-equilibrated hydrogels. The macroscopic morphology of PBS-equilibrated hydrogels is shown in Figure 1(B,D).

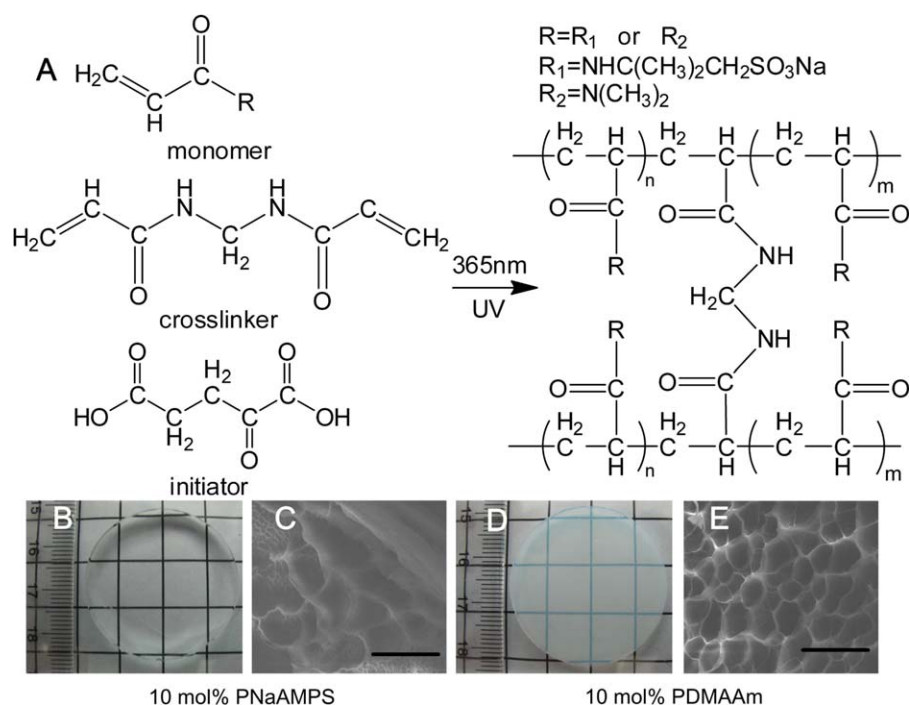


FIGURE 1. Hydrogel synthesis as well as macroscopic and microscopic morphology of hydrogels. A: Synthesis of PNaAMPS and PDMAAm hydrogels and the chemical structures of monomers, crosslinker (*N,N'*-methylenebisacrylamide), initiator (2-oxoglutaric acid), and crosslinked polymers. The hydrogels with chemical group R_1 or R_2 is PNaAMPS or PDMAAm hydrogel, respectively. B and D: The photos of PNaAMPS or PDMAAm hydrogels. C and E: SEM images of PNaAMPS or PDMAAm hydrogels (scale bar: 10 μm). All the samples were equilibrated in PBS. [Color figure can be viewed in the online issue, which is available at wileyonlinelibrary.com.]

Hydrogel characterization

Scanning electron microscopy. Samples were treated by the secondary freeze-drying operation (PowerDry LL1500, Thermo, USA) according previous procedures.²⁷ Scanning electron microscopy (SEM) images were obtained using scanning electron microscope (SEM, JEOL JSM-7000F, Japan). The microscopic morphology of PBS-equilibrated hydrogels observed by SEM is shown in Figure 1(C,E).

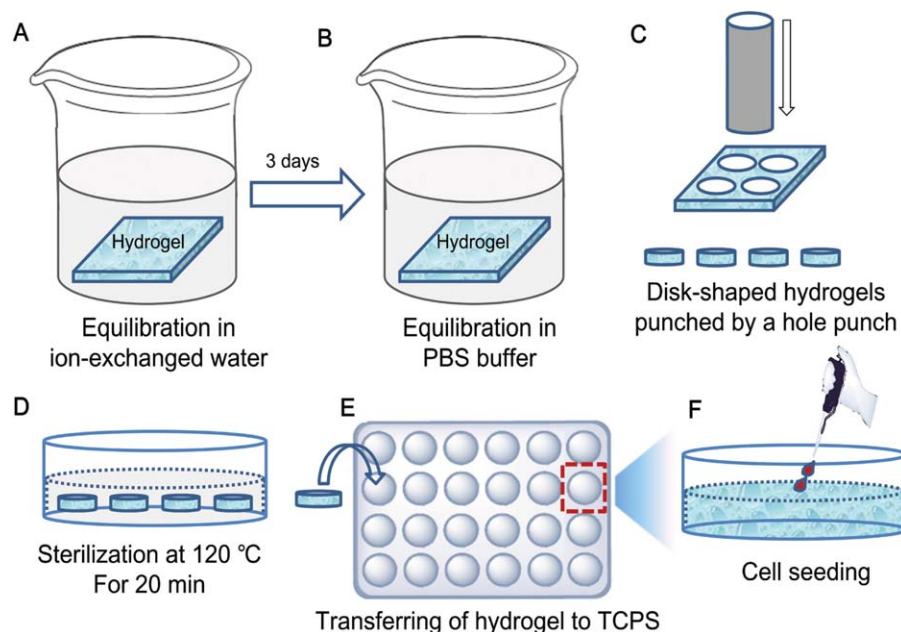
Degree of swelling. The degree of swelling (q) of hydrogel was quantified as the weight ratio of the swollen state (W_s) of hydrogel to that in the dry state (W_d), that is, $q = W_s/W_d$. q_{PBS} represents the degree of swelling of hydrogels equilibrated in PBS.

Young's modulus evaluation. The Young's modulus (E) of the hydrogel was tested by compressive stress-strain measurements using a tensile-compressive tester (CMT6503, MTS, USA). The prepared sheet-shaped hydrogels were punched into disk-shaped hydrogel samples (diameter is 15 mm and thickness is ca. 2–3 mm) by a hole punch. The samples were set on a lower plate, and then compressed with an upper plate at a strain rate of 10% min^{-1} at room temperature. E was determined by the average slope of stress-strain curve in the strain ratio range of 0.05 to 0.1,³⁶ and each value was averaged over four parallel measurements. E_{PBS} represents the Young's modulus of hydrogels equilibrated in PBS.

Protein adsorption. The amount of fibronectin adsorbed on the surface of PNaAMPS and PDMAAm hydrogels was quantitatively characterized via immunofluorescence as our previously reported protocol.²⁵ Sterilized PBS-equilibrated hydrogel disks with a diameter of 2.5 cm were exposed to 1.67 mL 20% FBS containing PBS buffer for 6 h at 37°C in a humidified atmosphere of 5% CO_2 . The same hydrogel disks blocked in 5% bovine serum albumin (BSA, Sigma) in PBS solution were used as controls. After rinsing with 1.67 mL PBS buffer for three times, the hydrogels were incubated with 1.67 mL 1:1000 dilution of FITC-conjugated anti-fibronectin (Biogenesis Ltd, UK) for 2 h at 37°C in a humidified atmosphere of 5% CO_2 . The immunostained samples were analyzed by a fluorescence confocal laser scanning microscope (OLYMPUS, Japan) after being washed three times with 1.67 mL PBS for three times. The fluorescence intensity difference between the hydrogels incubated in FBS and in BSA, which corresponded to the amount of adsorbed fibronectin on the hydrogel surfaces was detected.

Cell cultivation

The disk-shaped PBS-equilibrated hydrogels without modification by any cell-adhesive proteins or peptides were sterilized by autoclave (120°C, 20 min) in PBS and stored for cell culture. Process of cell cultivation was the same as previously described,^{37,38} and ARPE-19 cell line (ATCC Manassas, VA) was used for cell cultivation. DF-12 medium containing 10% (v/v) fetal bovine serum (Invitrogen,



SCHEME 1. Schematic representation of cell cultivation processes on the synthetic hydrogels without modification by cell-adhesive proteins or peptides. A: Sheet-shaped hydrogels are equilibrated in ion-exchanged water. B: Sheet-shaped hydrogels are equilibrated in PBS buffer. C: Disk-shaped PBS-equilibrated hydrogels are punched out of the sheet-shaped hydrogels by a hole punch. D: Disk-shaped PBS-equilibrated hydrogels are sterilized by autoclaving (120 °C, 20 min). E: The sterilized hydrogels are transferred into 24-well or 6-well TCPS. F: ARPE-19 cells are seeded on pure hydrogels. [Color figure can be viewed in the online issue, which is available at wileyonlinelibrary.com.]

Carlsbad, CA, USA), 0.348% sodium bicarbonate, 2 mM L-glutamine, 100 U/mL penicillin, and 100 U/mL streptomycin (Invitrogen, Carlsbad, CA, USA) was used for cell cultivation. The ARPE-19 cells were subcultured on the TCPS until confluent, and then were dissociated from the culture plate using 0.05% trypsin-EDTA (Invitrogen, Carlsbad, CA, USA) to obtain cell suspension. The hydrogel disks with 15 mm or 35 mm in diameter were transferred into a 24-well or 6-well tissue culture polystyrene (TCPS), respectively. The hydrogels with 15 mm in diameter were used for characterizing cell behaviors (adhesion, proliferation, monolayer formation, and morphology), and the hydrogel with 35 mm in diameter were used for ROS assay which needs a large amount of cells. The cell suspension with a density of 2.0×10^4 cells/mL was dropped onto the hydrogel surface. Then, ARPE-19 cells-seeded samples were cultured at 37 °C in a humidified atmosphere of 5% CO₂. The culture medium was changed every 48 h gently to avoid the damage of the cells and hydrogels. The morphology and proliferation of the cells cultured on the hydrogel substrate were monitored by taking photos using an phase contrast microscope (Olympus IX 71, Tokyo, Japan) equipped with a digital camera using 20× objectives at set time-points (6, 24, 48, 72, 96, and 120 h). Schematic representation of the processes of cell cultivation on the synthetic hydrogels is shown in Scheme 1.

Cell assay

live/dead assay. LIVE/DEAD Viability/Cytotoxicity Kit containing Calcein acetoxymethyl ester (Calcein AM) and Ethidium Homodimer 1 (EthD-1) (Molecular Probes, USA) was used to perform live/dead assay of cultured RPE cells to

evaluate the cytocompatibility of hydrogels. The images of the cell were visualized with fluorescence microscopy (OLYMPUS, Tokyo, Japan), and the numbers of live and dead cells were quantified using Image Pro Plus 6.0.

Fluorescence staining. For staining of cytoskeleton, rhodamine phalloidin (Enzo, America) was used according to the manufacture's introduction. To label the nuclei, the samples were stained with 0.1 mg/mL of 4',6-diamidino-2-phenylindole dihydrochloride (DAPI, Sigma-Aldrich, St. Louis, MO). The images of the F-actin and cell nuclei were obtained by Nikon C2 fluorescence confocal laser scanning microscopy (Nikon, Tokyo, Japan).

Intracellular ROS assay

Level of intracellular ROS was determined according to our previously reported protocol.^{38,39} Briefly, 10 μM 2',7'-dichlorodihydrofluorescein diacetate (DCFH-DA) (Sigma) was added to the cell monolayer-laden samples after cultivation for 120 h. The reduced form of DCFH-DA would be oxidized to the highly fluorescent dihydrochlorofluorescein (DCF) by ROS. The total amount of intracellular ROS production was obtained from the fluorescence intensity of the intracellularly trapped DCF measured by a plate reader (Fluoroskan Ascent, Thermo Fisher Scientific Inc. Waltham, MA) with an excitation of 485 nm and emission of 530 nm. To eliminate the influence of the cell number on the ROS assay, the total protein of cells cultured on the hydrogels was detected by BCA Protein Assay Kit (Beyotime, China).³⁸ The ROS value of the cells cultured on the hydrogels (ROS_{cell}) was denoted as the ratio of total ROS level (ROS_{total}) to total

amount of protein (P_{total}), that is., $ROS_{\text{cell}} = ROS_{\text{total}}/P_{\text{total}}$. Furthermore, the relative ROS level of cells cultured on the hydrogels (ROS_{RL}) was denoted as the ratio of ROS_{cell} to that of the control cells cultured on TCPS (ROS_{TCPS}), that is., $ROS_{\text{RL}} = ROS_{\text{cell}} / ROS_{\text{TCPS}}$.

Statistical analysis

The obtained data were expressed as mean \pm standard deviation at least over three samples (each in triplicate). Statistical significance was evaluated by using T-test. * p -values < 0.05 were considered statistically significant.

RESULTS AND DISCUSSION

Hydrogel properties

The physicochemical properties of hydrogels such as water content and stiffness are important for tissue engineering application. For instance, the hydrogel stiffness is particularly important for transplantation of RPE cell monolayer-hydrogel construct beneath retina and controlling over the surgical procedure. The surrounding soft tissues may be easily damaged if a hard substrate is implanted in subretinal space, whereas a too soft substrates is difficult to be operated in the surgical procedure.⁹ Therefore, the degree of swelling and Young's modulus (E) related to the water content and stiffness of hydrogel, respectively, were characterized and analyzed. In addition, the bulk solution for hydrogel equilibration has significant effects on hydrogel properties, because the osmosis pressure of hydrogel depends on the ionic strength of equilibrated solution.⁴⁰ Accordingly, hydrogel properties would be different when it is equilibrated in ion-exchanged water or PBS. Therefore, evaluation of hydrogel properties in PBS which ionic strength (0.15M) is similar to the cell cultivation medium is necessary for hydrogel potentially used in tissue engineering.

The degree of swelling of negatively charged PNaAMPS hydrogels with $C = 2$ mol %, 4 mol %, and 10 mol % equilibrated in PBS ($q_{\text{PBS}} = 38.7 \pm 1.7$, 27.3 ± 0.4 , 13.8 ± 0.5) were significantly higher than that of the neutral PDMAAm hydrogels with identical C ($q_{\text{PBS}} = 13.4 \pm 0.5$, 10.4 ± 0.2 , 8.2 ± 0.1) (Fig. 2). The results demonstrate that the anionic PNaAMPS hydrogels with sodium sulfonate groups in the pendant of their polymer chains enhance adsorption of more solution than neutral PDMAAm hydrogel without ionizable groups. In addition, the q_{PBS} of both PNaAMPS and PDMAAm hydrogels decreased with increasing C , whereas E_{PBS} of both PNaAMPS ($E_{\text{PBS}} = 5.0 \pm 0.2$ kPa, 24.0 ± 1.0 kPa, 169.3 ± 11.0 kPa) and PDMAAm ($E_{\text{PBS}} = 82.5 \pm 9.1$ kPa, 151.4 ± 24.3 kPa, 198.3 ± 6.8 kPa) hydrogels increased when $C = 2$ mol %, 4 mol %, and 10 mol %. The E_{PBS} of PNaAMPS hydrogels was lower than that of PDMAAm hydrogels when $C = 2$ mol % and 4 mol %, whereas the E_{PBS} of PNaAMPS hydrogel closed to that of PDMAAm hydrogel when $C = 10$ mol %. These results demonstrate that the Young's modulus of hydrogels less depend on charge density when C becomes large. We also checked the polymeric network structure of 10 mol % PNaAMPS and 10 mol % PDMAAm equilibrated in PBS using SEM. Because of the strong electrolyte properties of PNaAMPS, the mesh size

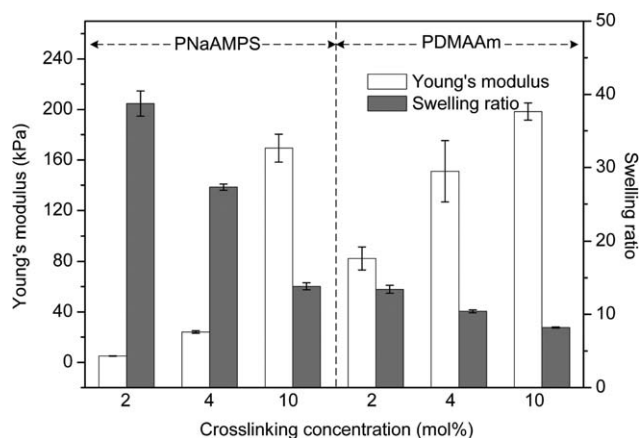


FIGURE 2. The degree of swelling (q) and Young's modulus (E) of hydrogels with various crosslinking concentration equilibrated in PBS. The white bar and gray bar represents Young's modulus and degree of swelling of hydrogels equilibrated in PBS, respectively. The numbers with unit in mol % are the crosslinking concentration in molar ratio in relative to monomer used in gelation. Error ranges are standard deviations over $n = 4$ samples.

of 10 mol % PNaAMPS hydrogel was obviously larger than that of 10 mol % PDMAAm hydrogel [Fig. 1(C,E)].

Cell proliferation

It is important that the RPE cells are transplanted as a monolayer beneath the retina, to avoid cell dysfunction including cell apoptosis and layered stacking, as well as to prevent postoperative complications including subretinal fibrosis and proliferative vitreoretinopathy.^{9,41} Therefore, we analyzed kinetic proliferation of the RPE cells cultured on PNaAMPS and PDMAAm hydrogels in long period cultivation. Comparing cell proliferation on the two kinds of hydrogels with different charge at 24 h and 120 h, we observed that significantly more RPE cells spread on the negatively charged PNaAMPS hydrogels than that on the neutral PDMAAm hydrogels (Fig. 3). This indicates the dramatically high kinetic proliferation of the RPE cells on the negatively charged PNaAMPS hydrogels. Besides, we observed that the cells cultured on all PNaAMPS hydrogels with $E_{\text{PBS}} = 5.0 \pm 0.2$ kPa, 24.0 ± 1.0 kPa, 169.3 ± 11.0 kPa appeared to have proliferated to monolayer with varied packing density at 120 h (Fig. 3). The results demonstrate that the RPE cells can proliferate and form monolayer on the PNaAMPS hydrogels regardless of charge over a wide range of Young's modulus ($E_{\text{PBS}} = 5.0$ – 169.3 kPa).

Comparing cell proliferation on the two kinds of hydrogels equilibrated in PBS with similar Young's modulus, that is., 10 mol % PNaAMPS ($E_{\text{PBS}} = 169.3 \pm 11.0$ kPa) as well as 4 mol % PDMAAm ($E_{\text{PBS}} = 151.4 \pm 24.3$ kPa) and 10 mol % PDMAAm ($E_{\text{PBS}} = 198.3 \pm 6.8$ kPa), the cells on the 169.3 kPa PNaAMPS hydrogel grew with culture time and proliferated to monolayer (Fig. 3) with a cell density of $4.43 \pm 0.7 \times 10^4$ cell/cm² at 120 h (Fig. 4). However, cells cultured on the 151.0 \pm 24.3 kPa and 198.3 \pm 6.8 kPa PDMAAm hydrogel could not proliferate and almost all cells died after 120 h cultivation.

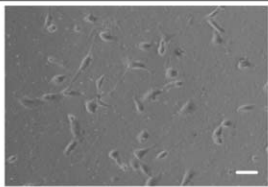
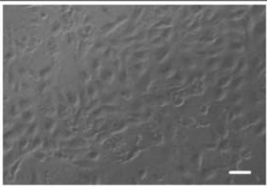
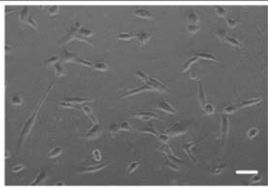
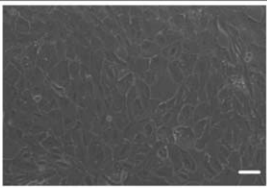
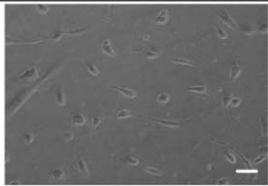
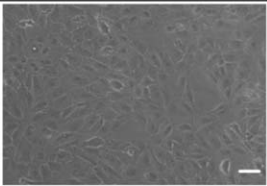
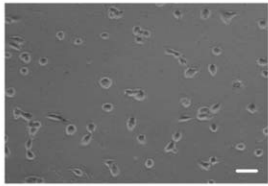
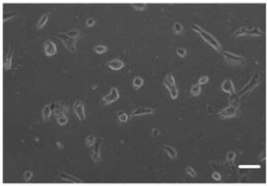
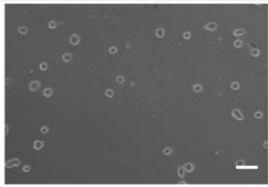
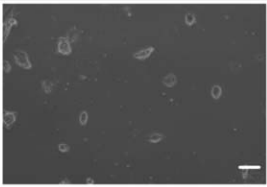
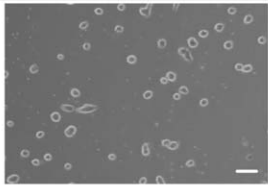
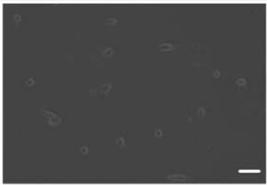
Hydrogel substrates			Cultivation time	
Monomer	C (mol%)	E (kPa)	24 h	120 h
NaAMPS	2	5.0 ± 0.2		
	4	24.0 ± 1.0		
	10	169.3 ± 11.0		
DMAAm	2	82.5 ± 9.1		
	4	151.4 ± 24.3		
	10	198.3 ± 6.8		

FIGURE 3. Phase-contrast micrographs of RPE cells cultured for 24 h and 120 h onto the surfaces of PNaAMPS and PDMAAm hydrogels with different crosslinking concentration (C , mol %) and Young's modulus (E , kPa) (scale bar: 50 μ m).

It is speculated that cell-adhesive proteins (fibronectin and vitronectin) contained in FBS play an important role in controlling anchorage-dependent cell behaviors.⁴² For example, fibronectin with arginine-glycine-aspartic acid (RGD) sequence for the binding of cell surface receptors plays a critical role in stimulation of anchorage dependent cells adhesion, spreading, and proliferation.²⁵ Therefore, the correlation between fibronectin adsorbed on hydrogel surface and cell behavior was further analyzed. It is demonstrated that high charge density in favor of fibronectin adsorption from the FBS contained in culture medium onto the surface of negatively charged hydrogels (Fig. 5), which further promoted RPE cells adhesion, spreading, and proliferation. On the other hand,

only a few fibronectin adsorbed onto neutral PDMAAm hydrogels, which resulted to inhibit RPE cell adhesion, spreading, and proliferation. The results agree with previous reports that negatively charged hydrogels promote spreading and proliferation of anchorage-dependent cells due to in favor of fibronectin adsorption.²⁵ However, neutral hydrogels with methacrylamide group does not facilitate RPE cell proliferation due to resistant to protein adsorption.⁴³

Evaluation of RPE cells grown on the PNaAMPS hydrogels

Live/dead assay. The live/dead assay was performed to check the viability of RPE cells of the monolayer cultured

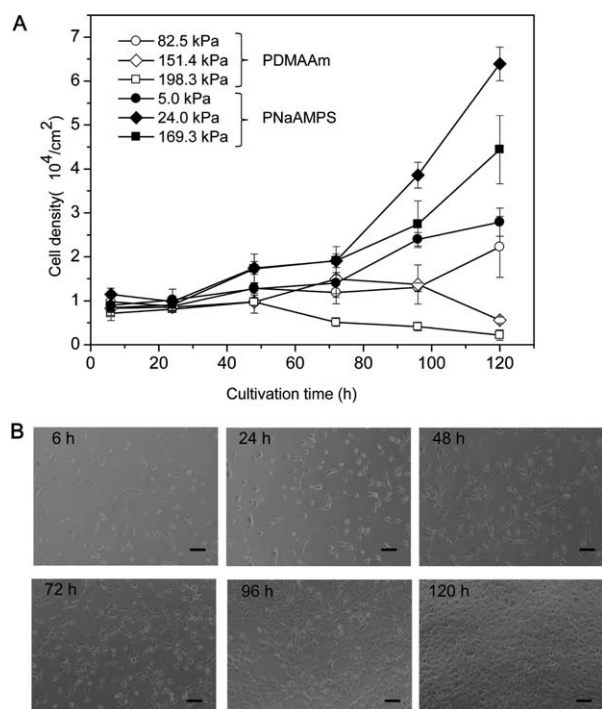


FIGURE 4. Proliferation of RPE cells on the PNaAMPS and PDMAAm hydrogels. A: Kinetic proliferation of the RPE cells cultured on surfaces of PNaAMPS hydrogels with Young's modulus of 5.0 ± 0.2 kPa (\bullet), 24.0 ± 1.0 kPa (\blacklozenge), 169.3 ± 11.0 kPa (\blacksquare), and PDMAAm hydrogels with Young's modulus of 82.5 ± 9.1 kPa (\circ), 151.4 ± 24.3 kPa (\diamond), 198.3 ± 6.8 kPa (\square). B: The phase-contrast micrographs of the cells cultured on PNaAMPS hydrogel with Young's modulus of 24.0 ± 1.0 kPa at different time point (scale bar: $100 \mu\text{m}$). Error ranges are standard deviations over $n = 4$ samples.

on PNaAMPS hydrogels with various Young's modulus. Viable cells stained with Calcein AM (green) and dead cells stained with EthD-1 (red) were observed in the phase-contrast fluorescence microscopy images (Fig. 6). After culturing for 72 h, the viable cells (green) greatly outnumber the dead cells (red), and the percentage of viable cells is

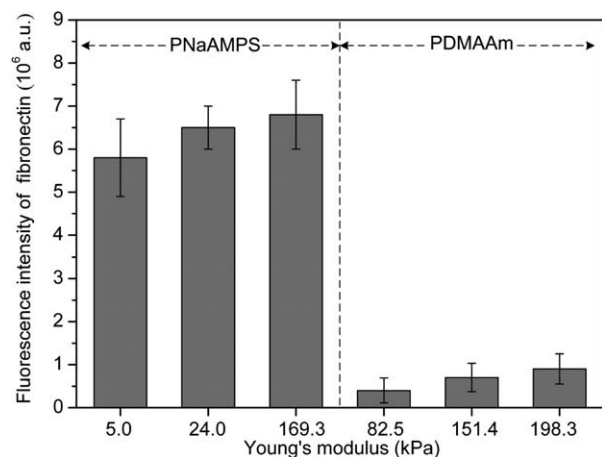


FIGURE 5. The fluorescence intensity of adsorbed fibronectin on hydrogels with various Young's modulus (E , kPa). No proteins were preadsorbed on the hydrogel surfaces before cell culture. Error ranges are the standard deviations over $n = 4$ samples.

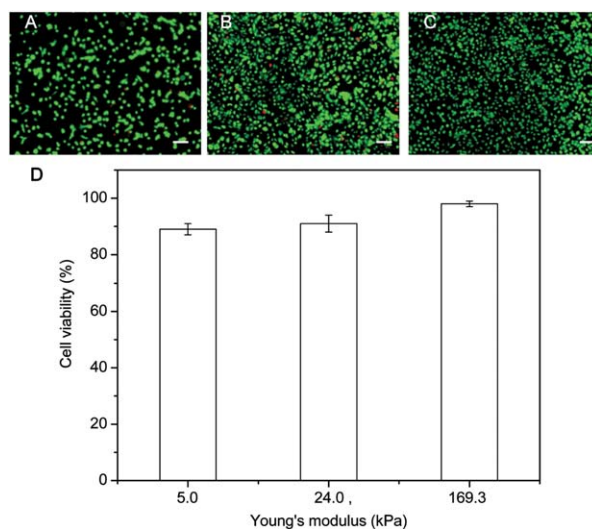


FIGURE 6. Viability of the RPE cells cultured on negatively charged PNaAMPS hydrogels detected by live/dead assay. RPE cells were cultured on PNaAMPS hydrogels with Young's modulus of 5.0 ± 0.2 kPa (A), 24.0 ± 1.0 kPa (B), 169.3 ± 11.0 kPa (C) for 72 h and then stained with live/dead reagents (scale bar: $50 \mu\text{m}$). A green fluorescence designates live cells, whereas a red fluorescence indicates dead cells. D: The cell viability obtained from the fluorescent images. Error ranges are standard deviations over $n = 4$ samples. [Color figure can be viewed in the online issue, which is available at wileyonlinelibrary.com.]

$89 \pm 2\%$, $91 \pm 3\%$, $98 \pm 1\%$ when E_{PBS} is 5.0 ± 0.2 kPa, 24.0 ± 1.0 kPa, 169.3 ± 11.0 kPa, respectively. The results indicate that RPE cells proliferate readily on the PNaAMPS hydrogels, and on the other hand, the good cytocompatibility of the hydrogel is proved.

Immunocytochemistry and cell cytoskeletal morphology. The cell monolayers cultured on the PNaAMPS hydrogels were stained with DAPI and Phalloidin-rhodamine to visualize the morphology of cell nucleus and cytoskeletal, respectively (Fig. 7). Formation of cell monolayer on the PNaAMPS hydrogels was supported by the distribution of DAPI staining cell nucleus observed from upper surface [Fig. 7(A-C)], and by the nuclei that did not overlap observed from vertical section [Fig. 7(J-L)]. The results demonstrate that the RPE cells grew to monolayer on the PNaAMPS hydrogels. Stress fiber organized by bundled filaments is a feature of normal strongly adherent RPE cells that are stationary on substrates.⁴⁴ Well-developed actin stress fibers distributed around individual cells and a complex networks formed by F-actin rings between cells were revealed by rhodamine phalloidin staining [Fig. 7(D-F)]. These results indicate that the RPE cells are well immobilized on the surfaces of PNaAMPS hydrogels.

ROS of RPE cells. RPE cells can easily become aging, and it has been reported that oxidative stress may play an important role in RPE dysfunction and degeneration. For instance, RPE cells may experience apoptosis due to the damage of mitochondrial DNA under sustained high level of ROS.^{19,45} Moreover, it is becoming increasingly clear that prevention

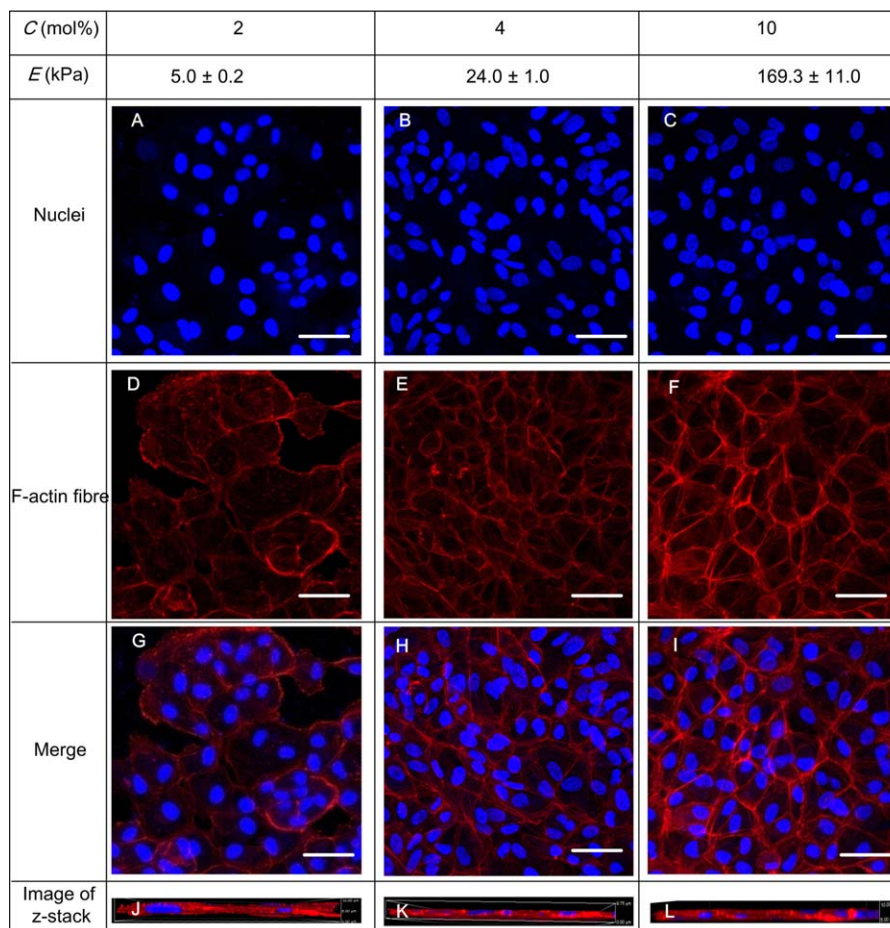


FIGURE 7. Morphology of the RPE cells following 120 h cultivation on PNaAMPS hydrogels with different Young's modulus (E , kPa). A, B, C: Nuclei revealed through staining with DAPI on the surface. D, E, F: F-actin fibres demonstrated by staining with rhodamine phalloidin. G, H, I: Merged photos of nuclei and F-actin fibres. J, K, L: Image of z-axis (scale bar: 100 μ m). [Color figure can be viewed in the online issue, which is available at wileyonlinelibrary.com.]

of RPE cells from oxidative damage should be focused on at early retinal diseases (e.g., ARMD) treatment stage.^{46,47} Therefore, it can be presumed that cultured RPE cells could exert its function better when being transplanted into the subretinal space if they have a relatively low ROS level.

Stiffness of hydrogel is a potential regulator that manipulates the behaviors and functions of cells. Recently, some researchers have reported that soft hydrogels can protect neurons from oxidative stress injury induced by hydrogen peroxide.⁴⁸ Therefore, it can be speculated that the hydrogel stiffness may also affect the ROS level of cultured RPE cells. To check this, we measured the ROS level of the RPE cells cultured on the PNaAMPS hydrogels as our previous reported methods.^{37,38} The data demonstrate that the intensity of the relative mean ROS level after forming cell monolayer (120 h) was reduced to 44% and 50% compared with control (the cells cultured on TCPS) on soft $E_{PBS} = 5.0 \pm 0.2$ kPa, 24.0 ± 1.0 kPa PNaAMPS hydrogels, respectively (Fig. 8). However, there was no significant difference of the ROS level between the cells cultured on the $E_{PBS} = 169.3 \pm 11.0$ kPa PNaAMPS hydrogel and control. This result indicates that the soft PNaAMPS hydrogels lead

to a significant decrease in intracellular ROS level compared to hard substrates. It was reported that hydrogels containing superoxide dismutase (SOD) mimetics or horseradish

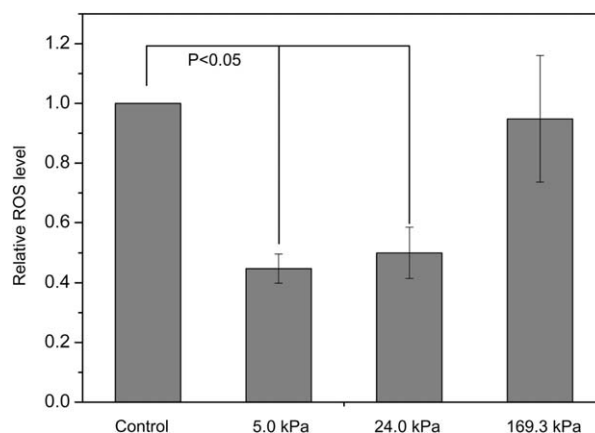


FIGURE 8. The relatively level of ROS on PNaAMPS hydrogels with different Young's modulus (E , kPa). $p < 0.05$ vs. the TCPS plates. Error ranges are standard deviations over $n = 4$ samples.

peroxidase inside could efficiently reduce ROS level.^{49,50} This is different from our experiments in which we used our hydrogel without modification by any enzyme as substrates for RPE cells cultivation. Although the exact mechanism of reduction of intracellular ROS production by soft hydrogels is unclear, identification of the molecular mechanisms facilitating RPE cells proliferate to monolayer with low ROS level on soft PNaAMPS hydrogel provides valuable information for regenerative RPE-based therapies. According to a recently published paper that indicated soft alginate hydrogels might protect neurons from oxidative stress injury via stimulation of cellular intrinsic antioxidant defenses, the most likely explanation is that the soft PNaAMPS hydrogels provided a more favorable microenvironment for RPE cells which could enhance cellular intrinsic antioxidant defenses to cope with the extra ROS.⁴⁸ In consideration of the fact, our next work will focus on the mechanism of soft hydrogels reducing the intracellular ROS. We will monitor the level of enzymatic molecules (i.e., SOD and horseradish peroxidase) and nonenzymatic molecules (i.e., vitamin E and vitamin C) correlating with reducing ROS to support our explanation.

In future, based on this investigation, a simple and economic approach can be used for harvesting functional RPE cell monolayer-hydrogel construct potentially candidate for regenerative RPE-based therapies, that is, the RPE cell monolayer with low ROS level can be obtained by simply culturing limited number of RPE cells obtained from donors on the soft PNaAMPS hydrogel films. There are a number of remaining challenges for implantation of RPE cell monolayer-PNaAMPS hydrogel construct in the subretinal space, such as preparation of a suitable thin hydrogel film (several tens of micrometers), testing of RPE survival and function by animal experiments *in vivo*.

In addition, since the PNaAMPS hydrogel facilitates both RPE cell and ECs growth, a 3D system constructed by RPE cell monolayer on the surface of PNaAMPS hydrogel substrate and EC capillary network into the substrate would be created and play a role as a graft of AMD implantation, or as an *in vitro* model for basic investigation of regenerative RPE-based therapies. In recent days, the functional hydrogels which could be used as scaffold for tissue engineering have attracted more and more attention, such as double network hydrogel^{29,35,51} and self-healing hydrogels.^{52,53} It could be presumed that a series of fascinating results could be obtained, if we combine these functional hydrogels with RPE cell cultivation in future.

CONCLUSIONS

This study demonstrates the feasibility of PNaAMPS hydrogel without modification by cell-adhesive proteins or peptides as a substrate for proliferation of RPE cell monolayer. Moreover, for the first time to our knowledge, it reveals that the ROS level of the cultured RPE cells is regulated by Young's modulus of PNaAMPS hydrogels, that is, the ROS level of the RPE cells cultured on the soft hydrogels (5.0 ± 0.2 kPa, 24.0 ± 1.0 kPa) obviously lower than that on

hard hydrogel (169.3 ± 11.0 kPa). Overall, it provides a more cost-effective soft biomaterial that shows great potential to be developed as an artificial substrate for RPE cell transplantation.

ACKNOWLEDGMENT

The authors thank doctor Ting Lei of cardiovascular research center, Xi'an Jiaotong University, for the help in operating fluorescence confocal laser scanning microscopy.

REFERENCES

- Cunningham ET Jr, Feiner L, Chung C, Tuomi L, Ehrlich JS. Incidence of retinal pigment epithelial tears after intravitreal ranibizumab injection for neovascular age-related macular degeneration. *Ophthalmology* 2011;118:2447–2452.
- Liao JL, Yu J, Huang K, Hu J, Diemer T, Ma Z, Dvash T, Yang XJ, Travis GH, Williams DS, et al. Molecular signature of primary retinal pigment epithelium and stem-cell-derived RPE cells. *Hum Mol Genet* 2010;19:4229–4238.
- Yaji N, Yamato M, Yang J, Okano T, Hori S. Transplantation of tissue-engineered retinal pigment epithelial cell sheets in a rabbit model. *Biomaterials* 2009;30:797–803.
- Rozanowska M, Bakker L, Boulton ME, Rozanowski B. Concentration dependence of vitamin C in combinations with vitamin E and zeaxanthin on light-induced toxicity to retinal pigment epithelial cells. *Photochem Photobiol* 2012;88:1408–1417.
- Stramm LE, Haskins ME, Aguirre GD. Retinal pigment epithelial glycosaminoglycan metabolism: Intracellular versus extracellular pathways. *In vitro studies in normal and diseased cells. Invest Ophthalmol Vis Sci* 1989;30:2118–2131.
- Ding JD, Johnson LV, Herrmann R, Farsiu S, Smith SG, Groelle M, Mace BE, Sullivan P, Jamison JA, Kelly U, et al. Anti-amyloid therapy protects against retinal pigmented epithelium damage and vision loss in a model of age-related macular degeneration. *Proc Natl Acad Sci USA* 2011;108:E279–E287.
- Hopley C, Salkeld G, Mitchell P. Cost utility of photodynamic therapy for predominantly classic neovascular age related macular degeneration. *Br J Ophthalmol* 2004;88:982–987.
- Seagle BL, Rezaei KA, Gasyna EM, Kobori Y, Rezaei KA, Norris JR Jr. Time-resolved detection of melanin free radicals quenching reactive oxygen species. *J Am Chem Soc* 2005;127:11220–11221.
- Singh S, Woerly S, McLaughlin BJ. Natural and artificial substrates for retinal pigment epithelial monolayer transplantation. *Biomaterials* 2001;22:3337–3343.
- Shadforth AM, George KA, Kwan AS, Chirila TV, Harkin DG. The cultivation of human retinal pigment epithelial cells on Bombyx mori silk fibroin. *Biomaterials* 2012;33:4110–4117.
- Lu L, Yaszemski MJ, Mikos AG. Retinal pigment epithelium engineering using synthetic biodegradable polymers. *Biomaterials* 2001;22:3345–3355.
- Geckil H, Xu F, Zhang X, Moon SJ, Demirci U. Engineering hydrogels as extracellular matrix mimics. *Nanomedicine* 2010;5:469–484.
- Seidi A, Ramalingam M, Elloumi-Hannachi I, Ostrovidov S, Khademhosseini A. Gradient biomaterials for soft-to-hard interface tissue engineering. *Acta Biomater* 2011;7:1441–1451.
- Lu JT, Lee CJ, Bent SF, Fishman HA, Sabelman EE. Thin collagen film scaffolds for retinal epithelial cell culture. *Biomaterials* 2007;28:1486–1494.
- Bhattacharya M, Malinen MM, Lauren P, Lou YR, Kuisma SW, Kanninen L, Lille M, Corlu A, GuGuen-Guillouzo C, Ikkala O, et al. Nanofibrillar cellulose hydrogel promotes three-dimensional liver cell culture. *J Control Release* 2012;164:291–298.
- Lai JY, Li YT. Influence of cross-linker concentration on the functionality of carbodiimide cross-linked gelatin membranes for retinal sheet carriers. *J Biomater Sci Polym Ed* 2010;22:277–295.
- Patenaude M, Hoare T. Injectable, degradable thermoresponsive poly (N-isopropylacrylamide) Hydrogels. *ACS Macro Lett* 2012;1:409–413.
- Turturro SB, Guthrie MJ, Appel AA, Drapala PW, Brey EM, Perez-Luna VH, Mieler WF, Kang-Mieler JJ. The effects of cross-linked

- thermo-responsive PNIPAAm-based hydrogel injection on retinal function. *Biomaterials* 2011;32:3620–3626.
19. Liang FQ, Godley BF. Oxidative stress-induced mitochondrial DNA damage in human retinal pigment epithelial cells: A possible mechanism for RPE aging and age-related macular degeneration. *Exp Eye Res* 2003;76:397–403.
 20. Hui S, Yi L, Fengling QL. Effects of light exposure and use of intraocular lens on retinal pigment epithelial cells in vitro. *Photochem Photobiol* 2009;85:966–969.
 21. Lu L, Hackett SF, Mincey A, Lai H, Campochiaro PA. Effects of different types of oxidative stress in RPE cells. *J Cell Physiol* 2006;206:119–125.
 22. Chen J, Patil S, Seal S, McGinnis JF. Rare earth nanoparticles prevent retinal degeneration induced by intracellular peroxides. *Nat Nanotechnol* 2006;1:142–150.
 23. Yang F, Williams CG, Wang DA, Lee H, Manson PN, Elisseff J. The effect of incorporating RGD adhesive peptide in polyethylene glycol diacrylate hydrogel on osteogenesis of bone marrow stromal cells. *Biomaterials* 2005;26:5991–5998.
 24. Schmidt J, Rowley J, Kong HJ. Hydrogels used for cell-based drug delivery. *J Biomed Mater Res A* 2008;87A:1113–1122.
 25. Chen YM, Ogawa R, Kakugo A, Osada Y, Gong JP. Dynamic cell behavior on synthetic hydrogels with different charge densities. *Soft Matter* 2009;5:1804–1811.
 26. Chen YM, Gong JP, Tanaka M, Yasuda K, Yamamoto S, Shimomura M, Osada Y. Tuning of cell proliferation on tough gels by critical charge effect. *J Biomed Mater Res A* 2009;88:74–83.
 27. Chen YM, Shiraishi N, Satokawa H, Kakugo A, Narita T, Gong JP, Osada Y, Yamamoto K, Ando J. Cultivation of endothelial cells on adhesive protein-free synthetic polymer gels. *Biomaterials* 2005;26:4588–4596.
 28. Chen YM, Tanaka M, Gong JP, Yasuda K, Yamamoto S, Shimomura M, Osada Y. Platelet adhesion to human umbilical vein endothelial cells cultured on anionic hydrogel scaffolds. *Biomaterials* 2007;28:1752–1760.
 29. Chen YM, Dong K, Liu ZQ, Xu F. Double network hydrogel with high mechanical strength: Performance, progress and future perspective. *Sci China: Technol Sci* 2012;55:2241–2254.
 30. Yang JJ, Chen YM, Liu JF, Kurokawa T, Gong JP. Spontaneous redifferentiation of dedifferentiated human articular chondrocytes on hydrogel surfaces. *Tissue Eng Part A* 2010;16:2529–2540.
 31. Kwon HJ, Yasuda K, Ohmiya Y, Honma K, Chen YM, Gong JP. In vitro differentiation of chondrogenic ATDC5 cells is enhanced by culturing on synthetic hydrogels with various charge densities. *Acta Biomater* 2010;6:494–501.
 32. Liu JF, Chen YM, Yang JJ, Kurokawa T, Kakugo A, Yamamoto K, Gong JP. Dynamic behavior and spontaneous differentiation of mouse embryoid bodies on hydrogel substrates of different surface charge and chemical structures. *Tissue Eng Part A* 2011;17:2343–2357.
 33. Ahmado A, Carr AJ, Vugler AA, Semo M, Gias C, Lawrence JM, Chen LL, Chen FK, Turowski P, da Cruz L, et al. Induction of differentiation by pyruvate and DMEM in the human retinal pigment epithelium cell line ARPE-19. *Invest Ophthalmol Vis Sci* 2011;52:7148–7159.
 34. Roehlecke C, Schaller A, Knels L, Funk RH. The influence of sublethal blue light exposure on human RPE cells. *Mol Vis* 2009;15:1929–1938.
 35. Gong JP, Katsuyama Y, Kurokawa T, Osada Y. Double-network hydrogels with extremely high mechanical strength. *Adv Mater* 2003;15:1155–1158.
 36. Parekh SH, Chatterjee K, Lin-Gibson S, Moore NM, Cicerone MT, Young MF, Simon CG. Modulus-driven differentiation of marrow stromal cells in 3D scaffolds that is independent of myosin-based cytoskeletal tension. *Biomaterials* 2011;32:2256–2264.
 37. Zhu L, Liu Z, Feng Z, Hao J, Shen W, Li X, Sun L, Sharman E, Wang Y, Wertz K, et al. Hydroxytyrosol protects against oxidative damage by simultaneous activation of mitochondrial biogenesis and phase II detoxifying enzyme systems in retinal pigment epithelial cells. *J Nutr Biochem* 2010;21:1089–1098.
 38. Feng Z, Liu Z, Li X, Jia H, Sun L, Tian C, Jia L, Liu J. α -Tocopherol is an effective Phase II enzyme inducer: protective effects on acrolein-induced oxidative stress and mitochondrial dysfunction in human retinal pigment epithelial cells. *J Nutr Biochem* 2010;21:1222–1231.
 39. Zou X, Feng Z, Li Y, Wang Y, Wertz K, Weber P, Fu Y, Liu J. Stimulation of GSH synthesis to prevent oxidative stress-induced apoptosis by hydroxytyrosol in human retinal pigment epithelial cells: activation of Nrf2 and JNK-p62/SQSTM1 pathways. *J Nutr Biochem* 2012;23:994–1006.
 40. Rubinstein M, Colby RH, Dobrynin AV, Joanny JF. Elastic modulus and equilibrium swelling of polyelectrolyte gels. *Macromolecules* 1996;29:398–406.
 41. Tezel TH, Del Priore LV. Reattachment to a substrate prevents apoptosis of human retinal pigment epithelium. *Graefes Arch Clin Exp Ophthalmol* 1997;235:41–47.
 42. Calonder C, Matthew HW, Van Tassel PR. Adsorbed layers of oriented fibronectin: A strategy to control cell-surface interactions. *J Biomed Mater Res A* 2005;75:316–323.
 43. Treharne AJ, Thomson HAJ, Grosse MC, Lotery AJ. Developing methacrylate-based copolymers as an artificial Bruch's membrane substitute. *J Biomed Mater Res A* 2012;100:2358–2364.
 44. Lee J, Ko M, Joo CK. Rho plays a key role in TGF- β 1-induced cytoskeletal rearrangement in human retinal pigment epithelium. *J Cell Physiol* 2008;216:520–526.
 45. Kalariya NM, Wills NK, Ramana KV, Srivastava SK, van Kuijk FJGM. Cadmium-induced apoptotic death of human retinal pigment epithelial cells is mediated by MAPK pathway. *Exp Eye Res* 2009;89:494–502.
 46. Wankun X, Wenzhen Y, Min Z, Weiyan Z, Huan C, Wei D, Lvzhen H, Xu Y, Xiaoxin L. Protective effect of paeoniflorin against oxidative stress in human retinal pigment epithelium in vitro. *Mol Vis* 2011;17:3512–3522.
 47. Chen YM, Liu JK, Feng ZH, Liu ZQ. Preparation of hydrogel scaffolds for promoting retinal pigment epithelium cells proliferation. *Chinese Patent* 2011. 201110191554.0.
 48. Matyash M, Despang F, Mandal R, Fiore D, Gelinsky M, Ikonomidou C. Novel soft alginate hydrogel strongly supports neurite growth and protects neurons against oxidative stress. *Tissue Eng Part A* 2012;18:55–66.
 49. Cheung CY, McCartney SJ, Anseth KS. Synthesis of polymerizable superoxide dismutase mimetics to reduce reactive oxygen species damage in transplanted biomedical devices. *Adv Funct Mater* 2008;18:3119–3126.
 50. Poulsen AK, Scharff-Poulsen AM, Olsen LF. Horseradish peroxidase embedded in polyacrylamide nanoparticles enables optical detection of reactive oxygen species. *Anal Biochem* 2007;366:29–36.
 51. Azuma C, Yasuda K, Tanabe Y, Taniguro H, Kanaya F, Nakayama A, Chen YM, Gong JP, Osada Y. Biodegradation of high-toughness double network hydrogels as potential materials for artificial cartilage. *J Biomed Mater Res* 2007; 81A:373–380.
 52. Dong K, Wei Z, Yang ZM, Chen YM. Self-healing gels: Structure, performance and future perspective. *Sci China: Chem* 2012;42:741–756.
 53. Yang B, Zhang YL, Zhang XY, Tao L, Li SX, Wei Y. Facilely prepared inexpensive and biocompatible self-healing hydrogel: A new injectable cell therapy carrier. *Polym Chem* 2012;3:3235–3238.